REPORT DOCUMENTATION PAGE

Form Approved
OMB No. 0704-0188

AD-A244 403

2. REPORT DATE	3. REPORT TYPE AND DATES COVERED
	ANNUAL 1 Dec 90 - 30 Nov 91

4. TITLE AND SUBTITLE
SOLAR VECTOR MAGNETIC FIELD RESEARCH

5. FUNDING NUMBERS
GR- AFOSR-90-0102
PE- 61102F
PR- 2311
TA- A1

6. AUTHOR(S)
Dr David M. Rust

7. PERFORMING ORGANIZATION NAME(S) AND ADDRESS(ES)
Applied Physics Laboratory
Johns Hopkins University
Johns Hopkins Road
Laurel, MD 20707-6099

8. PERFORMING ORGANIZATION REPORT NUMBER
81

9. SPONSORING/MONITORING AGENCY NAME(S) AND ADDRESS(ES)
Dr Henry R. Radoski
AFOSR/NL
Building 410
Bolling AFB DC 20332-6448

10. SPONSORING/MONITORING AGENCY REPORT NUMBER

11. SUPPLEMENTARY NOTES

12a. DISTRIBUTION/AVAILABILITY STATEMENT
Approved for public release;
distribution unlimited

12b. DISTRIBUTION CODE

13. ABSTRACT *(Maximum 200 words)*

Observations have been made before and after a large solar flare. Magnetic features were observed that could be used to predict flares it they are a regular feature of such events. The observations were among the first to show the development of shear within one hour of flare onset. Observations of linear polarization have been made of transient brightenings at small points in the lower chromosphere. The association between these flare-like events and magnetic fields has been studied. A feasibility study has been made of observing the sun with a balloon-borne vector magnetograph...The APL vector magnetograph developed under an OSR URI is operational.

92-01090

14. SUBJECT TERMS

15. NUMBER OF PAGES

16. PRICE CODE

17. SECURITY CLASSIFICATION OF REPORT	18. SECURITY CLASSIFICATION OF THIS PAGE	19. SECURITY CLASSIFICATION OF ABSTRACT	20. LIMITATION OF ABSTRACT
(UNCLASSIFIED)	(UNCLASSIFIED)	(UNCLASSIFIED)	(UNLIMITIED)

NSN 7540-01-280-5500

Standard Form 298 (Rev. 2-89)
Prescribed by ANSI Std. 239-18

92 1 13 015

Publications and presentations under Grant AFOSR-90-0102

PUBLICATIONS

D. M. Rust and J. W. O'Byrne, "Vector Magnetography," in *Solar Polarimetry* (L. November, ed.), National Solar Observatory, Sunspot, NM, p. 74.

D. M. Rust, "Solar Flares - An Overview, " *Advances in Space Research* (in press).

D. M. Rust, "Sociology of the SMY," *Advances in Space Research* **11**, 123.

D. M. Rust, "The Earth's Climate and the Variability of the Sun over Recent Millennia," (book review) *EOS Transactions* **72**, 157.

D. M. Rust and S. L Keil, "A Search for Polarization in Ellerman Bombs," submitted to *Solar Physics.*

PRESENTATIONS

G. Cauzzi (AFSC/PL, D. M. Rust, and J. W. O'Byrne (University of Sydney, "A New Method for Calibrating Vector Magnetograms", presented at the Twenty-First Meeting, American Astronomical Society Solar Physics Division, April 9-11, 1991, Huntsville, Alabama.

D. M. Rust, "Etalon Filters," presented at the Workshop on Focal Plane Instrumentation for LEST, Huntsville, Alabama, April 8, 1991.

D. M. Rust, "A Search for Polarization in Ellerman Bombs", presented at the Twenty-First Meeting, American Astronomical Society Solar Physics Division, April 9-11, 1991, Huntsville, Alabama.

D. M. Rust, "Plans for a Balloon-Borne Vector Magnetograph", presented at the U.S. - Taiwan Bilateral Workshop on Solar Variability Effect on the Atmosphere and Space Processing", Taiwan, April 16, 1991.

D. M. Rust, "The Case for a Vector Magnetograph", Responses for the Meeting on the SEON Upgrade: Vector Magnetograph Operational Requirements and Concepts, April 25-26, 1991, National Solar Observatory, Sunspot, NM.

D. M. Rust, "Searching for the Origins of Solar Flares", presented to the Westminster Astronomical Society of Maryland at Western Maryland College, Westminster, July 17, 1991.

D. M. Rust and G. Cauzzi, "New Vector Magnetograph Studies Active Regions", presented at the International Astronomical Union General Assembly, Buenos Aires, Argentina, July 29, 1991.

D. M. Rust and G. Cauzzi, "Variation of the Magnetic Field Vector in An Eruptive Flare", IAU Colloq. 133, Iquazu, Argentina, August 2, 1991.

A SEARCH FOR POLARIZATION IN ELLERMAN BOMBS

David M. Rust

The Johns Hopkins University Applied Physics Laboratory
Laurel, MD 20723 U.S.A.

and

Steven L. Keil

U. S. Air Force Phillips Laboratory
Sacramento Peak Observatory
Sunspot, New Mexico 88349

Abstract. Ellerman bombs, also called 'moustaches', are transient brightenings at tiny (< 1 arcsec) points in the lower chromosphere whose spectra are characterized by very thin and elongated emission wings on the hydrogen Balmer lines. Babin and Koval recently found linear polarization as high as 20% in bombs, but no physical process that could produce such a high degree of polarization was suggested. A new observational study of polarization in Ellerman bombs is reported here. Images of 32 bombs were obtained with a digital video system viewing the sun through a 6 Å filter at the Sacramento Peak Vacuum Tower Telescope. A novel polarizing beamsplitter divided each image into two interleaved polarized components which passed simultaneously through a single set of optics and were separated only during data analysis. The sensitivity threshold of the measurements was ~ 1%. In 4 cases out of 32, linear polarization above 2% was detected. The higher incidence of > 2% polarization reported by Babin and Koval is not confirmed.

submitted to Solar Physics

1. Introduction

Ellerman bombs (Ellerman, 1917) are transient brightenings at tiny (< 1 arcsec) points in the lower chromosphere. A typical bomb lasts about 10 minutes. Its spectrum is characterized by greatly elongated emission wings on the hydrogen Balmer lines (Severny and Koval, 1961). On a photographic negative, the pattern of a bomb's emission resembles a moustache or whisker, and these terms are used frequently in the solar literature. We will use 'moustache' when discussing the spectra of bombs.

Moustaches apparently occur below $\tau_{5000} = 0.4$ (Severny, 1964). Their enhanced emission does not extend into the hydrogen line cores. Emission at line center is lacking presumably because of absorption in the overlying atmosphere or in the moustache itself. This is an important difference from flares: all flares are brightest in the cores of the affected lines. In flares the chromosphere is heated from the overlying corona. The uppermost layers are affected first, whereas the moustaches imply that the heating originates in the low chromosphere (Kitai 1983).

We report here an observational study of polarization in Ellerman bombs. Babin and Koval (1985, 1986, 1987) found as much as 20% linear polarization either aligned with arch filament system fibrils or perpendicular to the limbward direction. They did not suggest a physical process that could produce such a high degree of polarization in the low chromosphere, especially in the far wings of the H_α line. The mechanism of impact polarization invoked by Hénoux *et al.* (1990) to explain weak polarization observed at line center in some H_α flares does not seem applicable here. Impact polarization is caused by high-energy protons beamed from the corona.

Bombs are interesting because of their close association with the boundaries of magnetic field concentrations (Koval, 1965, Roy, 1973) and the resemblance of their extended emission wings to those found in some solar flares. Bombs are almost always seen in emerging flux regions (Bruzek, 1967) and at the outer edges of sunspot

penumbrae, where flux cancellation occurs (Martin and Rust, 1991). They share this property with solar flares, so a study of bombs may shed light on the flare mechanism.

Because so little has been published recently about Ellerman bombs, we review their properties (§ 2). In § 3, we describe a novel polarizing beamsplitter and the experimental and data analysis procedures used to infer the degree of linear polarization. In § 4, we describe the results of our first measurements. Finally, in § 5, we comment on discrepancies between our results and those of Babin and Koval.

2. Ellerman Bomb Properties

Ellerman bombs coincide with continuum facular granules (Bruzek 1972; Kitai and Muller 1984). They also coincide with the bright points seen at 3840 Å (Vorpahl and Pope (1972). These bright points correspond, in turn, to magnetic flux elements. They are associated with the formation of sunspots. According to Vorpahl and Pope, the bright points appear before the first dark spot. In the best 3840 Å filtergrams, bright features composed of elements < 700 km diam can be seen drifting outward from sunspot pores (Vorpahl and Pope (1972). They are the same as moving magnetic features. Martin and Rust (1991) found that bombs occur where magnetic features of one polarity meet other, opposite polarity features. Roy (1973) found that bombs occur only where the magnetic fields are changing and estimated the average rate of flux change at 3×10^{15} Mx s^{-1}. Bomb frequency and number increase with growth rate of the magnetic field. Rust (1968) suggested that bombs occur at magnetic field reconnection points. Kitai (1983) suggested instead that bombs occur in isolated flux tubes.

According to Vorpahl and Pope, 3840 Å brightness enhancements at bomb sites lead H_α bomb onset by 3.5 min, and they last 20 - 94 min versus 7 - 64 min for the H_α bombs. When bombs occur in clusters, they attain maximum brightness within 2 - 3 min of each other.

Bomb visibility does not depend on distance from the limb. Kurokawa *et al.* (1982) studied bombs at H_α - 1.2 Å near the solar limb and found them elongated in the radial direction. The mean length was 800 km, the mean width 350 km, but the seeing may have determined the size. The mean lifetime of Kurokawa's bombs was 12 min, in good agreement with the 11-min lifetime found by Roy and Leparskas (1973). Some bombs lasted much longer but all of them pulsated. Recurrence of bombs in the same location is common. Also, maximum brightness and maximum length are achieved at nearly the same time, but bombs grow only in length at first. Kurokawa *et al.* estimated a mean upward velocity of 8 km s^{-1} during the first 2 min of bomb development and pointed out that this could account for the blue asymmetry in moustaches (Severny, 1968). Kitai (1983) gave upward velocities of 1 km s^{-1} in the photosphere and 6 km s^{-1} in the chromosphere.

Roy and Leparskas (1973) found that H_α surges originate in bombs, and that surge length (amount of material) is proportional to bomb size times the lifetime. The surges they studied consisted of clusters of very fine dark (sometimes bright) filaments connected to the bombs. The trajectories of the surge threads above 5000 km matched lines of force calculated in the current-free approximation.

Moustaches are about 10% brighter than the continuum 1 Å from H_α line center. Severny was the first to study the spectra of moustaches extensively, and Severny and Koval (1961) showed that Stark broadening cannot explain the extended line wings. Engvold and Maltby (1968) measured moustache profiles, finding line widths ranging from 3 to 10 Å. The true widths could have been greater, having escaped detection because of instrumental dilution.

Engvold and Maltby estimated there are ~ 100 moustaches per spot group. The spectra are usually asymmetrical, with 60% being brighter in the blue and 40% brighter in the red. But the asymmetry could be due to the effect of overlying material. Engvold and Maltby suggest that the true moustache profile is symmetric.

Severny and Khokhlova (1958) found weak linear polarization in moustaches. Babin and Koval, also at the Crimean Astrophysical Observatory, have carried on the work, in one instance finding 24% linear polarization (Babin and Koval, 1987) in the enhanced emission. They subtracted an estimated background from the bomb brightness before computing the polarization degree. From a study of H_α spectra taken simultaneously at four linear polarizations, Babin and Koval concluded that the degree of linear polarization in any given moustache is the same over the entire emission contour but the orientation of the plane of polarization may be different for adjacent moustaches, and some large moustaches encompass differently polarized elements. Generally, they say the electric vector is perpendicular to the radial direction on the solar disk.

3. Experimental Method

The objective of our experiment, which is sketched in Figure 1, was to obtain simultaneous measurements of orthogonal polarization states with a narrow-band filter. We tried to obtain high resolution over a field of view that would include many bombs. Such filter observations have advantages over spectrographic ones, *e.g.*, it is easier to study the temporal development of many bombs at once. We were only partially successful in the observing run reported here. Better seeing conditions will be necessary to resolve most of the smaller bombs and to follow their evolution.

The first optical element in the setup was the Vacuum Tower Telescope (VTT) at the Sacramento Peak Observatory, the F/72 beam of which produces a 500-mm diameter solar image. Before the primary focus, the beam passed through a halfwave plate P1 and a field lens F1. A mask admitted a section of the image, about 50 arcsec square, to the 125-mm (focal length) relay lens O1. At the prime focus, we placed a Ronchi ruling (10 lp mm^{-1}) that was cemented to a 16-mm diameter wafer of crystalline lithium niobate. The crystal was cut so that the faces of the wafer were 45° to the optical axis.

Lithium niobate is birefringent, so light passing through the wafer was divided into two oppositely-polarized beams, shown in Figure 2 as $\mathcal{P}$ and $\mathcal{S}$. The thickness of the

wafer was 1.35 mm, just enough to produce a 50-μm lateral displacement in the extraordinary beam. That displacement matched the pitch of the rulings and produced simultaneous, interlaced polarized images.

The beam-interleaving polarization analyzer sacrificed half the available light, because of the opaque rulings, and the spatial sampling rate perpendicular to the ruling direction was half of that in the parallel diection, but the two beams followed almost identical paths and were sensed simultaneously by the same detector array. The image scale at the ruling was 0.4 arcsec lp^{-1}, so.the width of the sampling slits was only 0.2 arcsec, but the spatial resolution - twice the sample interval - was 0.8 arcsec. The seeing would rarely justify use of higher resolution than this.

A videcon camera system digitized the images in 500 *x* 500-pixel arrays with 8-bit precision. The system measured the rms intensity contrast for each of the 30 video frames produced each second and saved only the frame with the highest contrast in each 1-s interval. Each video frame was composed of two interlaced 'fields'. The seeing for the two fields could have differed slightly because of a 0.0167-s difference in record times.

Magnification by the O1 lens was adjusted to allot three rows of video pixels to each 50-μm slit at the primary solar image. In practice, it proved impossible to obtain the exact magnification to place the $\mathcal{P}$-polarized light (Figure 2) on each odd triplet of pixels and the $\mathcal{S}$-polarized light on each even triplet. The slight difference in pitch between the re-imaged slits and the rows of pixels, as well as local variations in image scale (due possibly to non-uniformity of the videcon) had to be corrected in the data analysis program.

As shown in Figure 1, the beam passed through a 6-Å thin-film interference filter and, during calibration, a polaroid filter. For calibration, a series of images was obtained while the polaroid was rotated through 90°. The images showing maximum contrast between adjacent triplets of pixels gave the system response to 100% polarization. For data analysis, these calibration images formed a mask that allowed separation of the video frames into $\mathcal{P}$ and $\mathcal{S}$ images. During some of the observations a half-wave plate was

inserted in the beam in front of the Ronchi ruling and beamsplitter. This wave-plate was rotated 45° from one image sequence to the next, and the resultant data were examined for differences between the 0° position and the 45° position. The effect of rotating the waveplate was to reverse the phase of the signal on the $\mathcal{P}$ and $\mathcal{S}$ row-triplets. The detector response ("gain") of each pixel was found from images obtained during random-path scans of the solar image.

Figure 3 plots the intensities along a vertical cut through the bands formed when the polaroid was in the beam. The $\mathcal{P}$ and $\mathcal{S}$ images were constructed from the middle row of pixels in each white and black band, respectively, corresponding to the maxima and minima, shown in the plot.

After correcting the $\mathcal{P}$ and $\mathcal{S}$ images for gain, we applied a destretching routine, based on local correlation tracking techniques, to eliminate false signals arising from atmospheric seeing differences. Figure 4 shows the interlaced $\mathcal{P}$ and $\mathcal{S}$ images and the same images after separation and gain correction.

The destretched $\mathcal{P}$ and $\mathcal{S}$ images were used to compute the percentage of linear polarization present in each bomb. Subtracting the $\mathcal{P}$ from the $\mathcal{S}$ images gave a signal proportional to the amount of linear polarization, including both solar and instrumental sources.

Let I'_p and I'_s be the observed intensity in the $\mathcal{P}$ and $\mathcal{S}$ image respectively. The calibration frames show that if light that is 100% linearly polarized in either the $\mathcal{P}$ or $\mathcal{S}$ plane is introduced into the system, the video detector produced a saturated signal (255) in one channel and a null (0) in the other. This is the system response to 100% polarization. Computing

$$M' = (I'_p - I'_s)/(I'_p + I'_s - 2\,I'_{ph}) \qquad (1)$$

yielded a polarization signal M' of either 1.0 or -1.0 for light 100% polarized along the $\mathcal{P}$ or $\mathcal{S}$ channel, respectively, and 0 for unpolarized light, circularly polarized light, or for 100% linearly polarized light coming in at exactly 45° to the $\mathcal{P}$ and $\mathcal{S}$ planes. That is, we

measured linear polarization only to the degree that it was resolved along the $\mathcal{P}$ or $\mathcal{S}$ planes, hence our measurements will underestimate the polarization that may be present on the sun.

Instrumentally-induced or some other systematic polarization usually offset the polarization signal M' from zero. Figure 5 shows histograms of M' for 12 different fields of view, each of which contained Ellerman bombs that occupied only a tiny fraction of the scene area. The histograms show that the systematic polarization signal was never more than 1% or 2%. The histograms also show that the maximum polarization signals before correction for background were just a few percent.

We removed the unpolarized background before computing the percentage of polarization in the bombs. After correcting each bomb image for the background level of the surrounding photosphere, *i.e.*, finding $I_p = I'_p - I'_{ph}$ and $I_s = I'_s - I'_{ph}$, we computed the polarization M in each bomb:

$$M = (I_p - I_s)/(I_p + I_s). \qquad (2)$$

where I'_{ph} is the background photospheric intensity. The corrected polarization signal, M, could only be measured in regions brighter (or darker) than the continuum, since I_p and I_s were quite small for unpolarized light at continuum intensities, so M became very large and noisy. The Ellerman Bombs varied in intensity from about 10% to about 30% brighter than the continuum. We measured the polarization only for those bombs with $I'_{bomb} > 1.10\ I'_{ph}$.

4. Results

On 2 August 1990 there was a very rich field of Ellerman bombs in NOAA region 6172 at S25W43 (radius vector of 0.8 R$_\odot$). This region had been stable for four days before 1 August. Then, in 24 hours, the total area of the spots increased from 50 millionths of the solar hemisphere to 500 millionths. The spots increased from 540 millionths to 890 in the 24 hours after our observations. Such rapid growth in a region usually produces a large number of Ellerman bombs.

We measured twelve somewhat overlapping locations near the spots, and each 50 arcsec-square field had one or more very bright Ellerman bombs. Occasional moments of very good seeing revealed many more bombs too faint to show up in the summed images. Either 20 or 120 video images were recorded and summed at each location, each image having been automatically selected as the best of 30 images in a 1-s interval. The $\mathcal{P}$ images were destretched with the corresponding $\mathcal{S}$ images as the reference, and for each pair, a map of M was produced, giving 20 or 120 polarization maps at each location. These maps were aligned, then summed to form a mean polarization map. The individual maps were used to calculate the rms noise level.

In the 20 to 120 s interval covered by the individual polarization measurements, only a small evolutionary change in the solar magnetic field is expected. Thus, the variance between frames can be used to estimate the uncertainty in determining the polarization. The rms variance at a given point in the bomb was typically equal to about one third of the signal for the more polarized bombs and about half the signal in the weaker bombs.

Figure 6 shows the intensity images at five bomb regions and the corresponding polarization maps. We computed the rms fluctuations in polarization at all points in the bombs (generally defined as $I > 1.10\, I_{ph}$). The sensitivity of the measurements in the bombs was 1 - 2%.

Thirty-two bombs were observed in 75 min. One bomb had 8% polarization, one 5% and two 4%. Nineteen registered 2% ± 1%, and nine were less than 2% linearly polarized. The polarization was usually uniform, but one large bomb was 2% polarized in the center and 5% polarized in a ring about the center. In location No. 8 there were seven closely-spaced bombs, and most had two lobes, oppositely polarized at 2%.

In summary, linear polarization in 28 out of 32 bombs was just above the detection threshold or below it. We cannot confirm the high levels of polarization reported by Babin and Koval. But in a few instances, we find 4 - 8% polarization, and we find some bombs with several differently polarized elements, as did Babin and Koval.

5. Discussion

Our technique for measuring linear polarization differs from those used by Babin and Koval in several respects. It differs from their 1986 work with an H_α filter since images at the two orthogonal senses of polarization were obtained very nearly simultaneously, *i.e.*, within one $1/30^{th}$-s video frame cycle. The importance of obtaining simultaneous images for the study of such tiny features and of registering them precisely cannot be overstated. In their work with filtergrams, Babin and Koval had to subtract single image pairs taken several seconds apart. We feel, and Babin and Koval (1987) seem to agree, that since the brightness of bombs varies rapidly this procedure could seriously affect the measurements. A more serious problem was posed, no doubt, by variations in bomb brightness and position caused by changing image quality.

Our observations were obtained with a 6 Å thin-film interference filter centered on H_α whereas in their 1987 work, Babin and Koval used a spectrograph. It is conceivable that the true polarization in bombs varies with wavelength and that our wide filter allowed the polarization to average to nearly zero. However, our results are still inconsistent with Babin and Koval (1987) because they claim that the degree and direction of polarization does not depend on wavelength. We intend to check this point in future observations with a tunable filter.

We considered the possibility that our 6 Å filter produced an undesirable dilution of the bomb emission, but the bombs in our images are ~ 10% brighter than the background, consistent with most other measurements. The apparent size of the smallest bomb in our survey was ~ 2 arcsec, but Kurokawa *et al.* (1982) found a mean length of only 1 arcsec and a mean width of 1/2 arcsec. We did select only the largest bombs for study, but better images would allow for a better determination of the potential effects of dilution.

Both we and Babin and Koval subtracted the estimated background intensity from the observed $\mathcal{P}$ and $\mathcal{S}$ intensities I'_p and I'_s. If the emission is indeed optically thin and/or the filling factor is small, then subtraction of the underlying emission is appropriate to find

the degree of polarization. However, if bombs are opaque and the filling factor is near unity, then subtraction of a 'background' leads to indicated polarization levels that depend irrelevantly on the brightness of the bomb relative to the background. The indicated polarization could then be much higher than the true polarization.

Babin and Koval claim that instances of strong polarization are short-lived, so it is conceivable that we were almost never in the right place at the right time to measure high levels of polarization similar to what they report. Or, perhaps our 20 - 120-s integrations were too long. If the average polarization in a bomb were ~ 10%, then we should have seen more cases of polarization over 2%. Babin and Koval report 31 positive detections, all of at least 2% polarization. They report only six instances of less than 5% polarization. They do not say what their detection threshold was or in what percentage of cases they found no polarization.

We will make more observations, under better seeing conditions we hope, and we will systematically rotate the $\lambda/2$ plate in 22 1/2° steps. The present work leaves open the possibility that the axes of our detector were close to 45° from the electric vector in the bombs.

Acknowledgements

DMR's work was sponsored by the Air Force Office of Scientific Research Grant 90-0102.

References

Babin, A. N. and Koval, A. N.: 1986, *Izv. Krim. Astrofiz. Obs.* **75**, 52.

Babin, A. N. and Koval, A. N.: 1987, *Izv. Krim. Astrofiz. Obs.* **77**, 9.

Bruzek, A.: 1967, *Solar Phys.* **2**, 451.

Bruzek, A.: 1972, *Solar Phys.* **26**, 94.

Ellerman, F.: 1917, *Astrophys. J.* **45**, 298.

Engvold, O. and Maltby, P.: 1968, in *Mass Motions in Solar Flares and Related Phenomena* (Y. Ohman, ed.), Wiley, London, p. 109.

Hénoux, J. C., Chambe, G., Smith, D., Tamres, D., Feautrier, N., Rovira, M., and Sahal-Bréchot, S.: 1990, *Astrophys. J. Suppl.* **73**, 303.

Kitai, R.: 1983, *Solar Phys.* **87**, 135.

Kitai, R. and Muller, R.: 1984, *Solar Phys.* **90**, 303.

Koval, A. N.: 1965, *Izv. Krim. Astrofiz. Obs.* **34**, 278

Koval, A. N. and Severny, A. B.: 1956, *Astron. Zh.* **33**, 74.

Kurokawa, H., Kawaguchi, I., Funakoshi, Y., and Nakai, Y.: 1982, *Solar Phys.* **79**, 77.

Martin, S. F. and Rust, D. M., in preparation.

Roy, J.-R.: 1973, Ph.D. Thesis, University of Western Ontario, London, Canada.

Roy, J.-R. and Leparskas, H.: 1973, *Solar Phys.* **30**, 449.

Rust, D. M.: 1968, in K. O. Kiepenheuer (ed.), "Structure and Development of Solar Active Regions," *IAU Symp.* **35**, 77.

Severny, A. B.: 1964, *Ann. Rev. Astron. Astrophys.* **2**, 363.

Severny, A. B. and Khokhlova, V. L.: 1958, *Izv. Krymsk. Astrofiz. Obs.* **20**, 68.

Severny, A. B. and Koval, A. N.: 1961, *Izv. Krymsk. Astrofiz. Obs.* **26**, 3.

Vorphal, J. and Pope, T.: 1972, *Solar Phys.* **25**, 347.

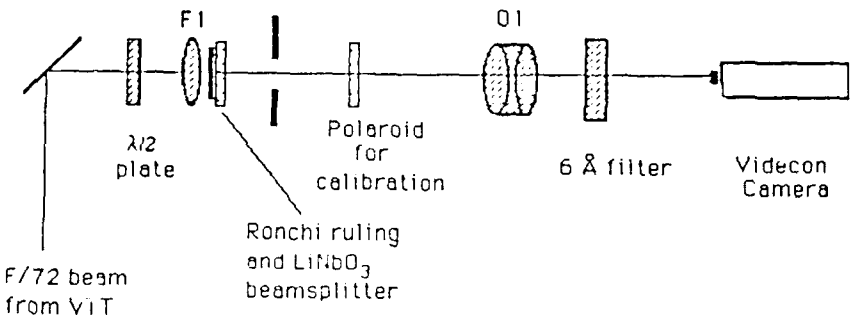

Fig. 1. Experimental setup for measuring polarization at the Vacuum Tower Telescope. F1 is a field lens; O1 is a 125-mm 1:1 reimaging lens. The polaroid was used only for calibrations.

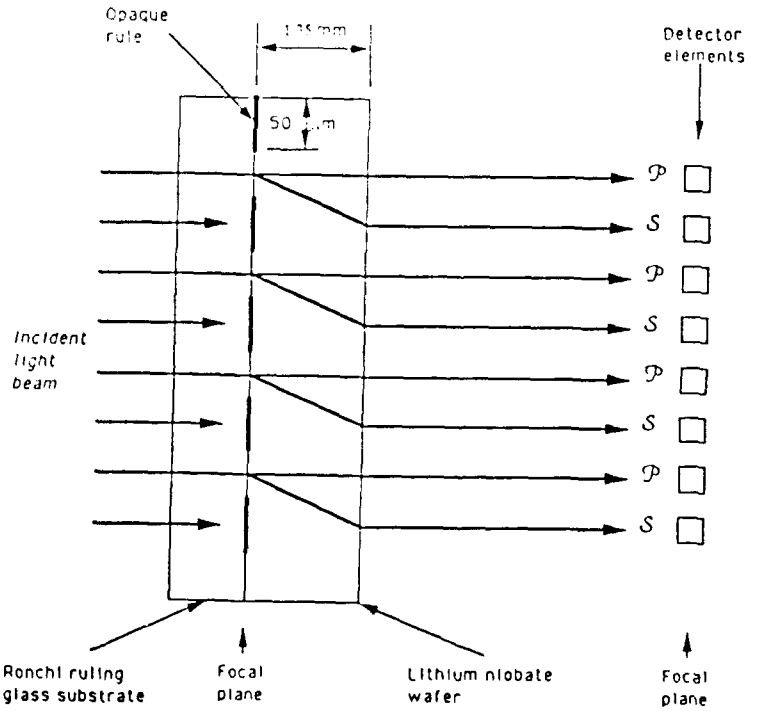

Fig. 2. The beam-interleaving polarization analyzer. The wafer faces are 45° to the optic axis of the lithium niobate, so that the *S* beam is offset by one 50 μm rule width. The reimaging optics are not shown.

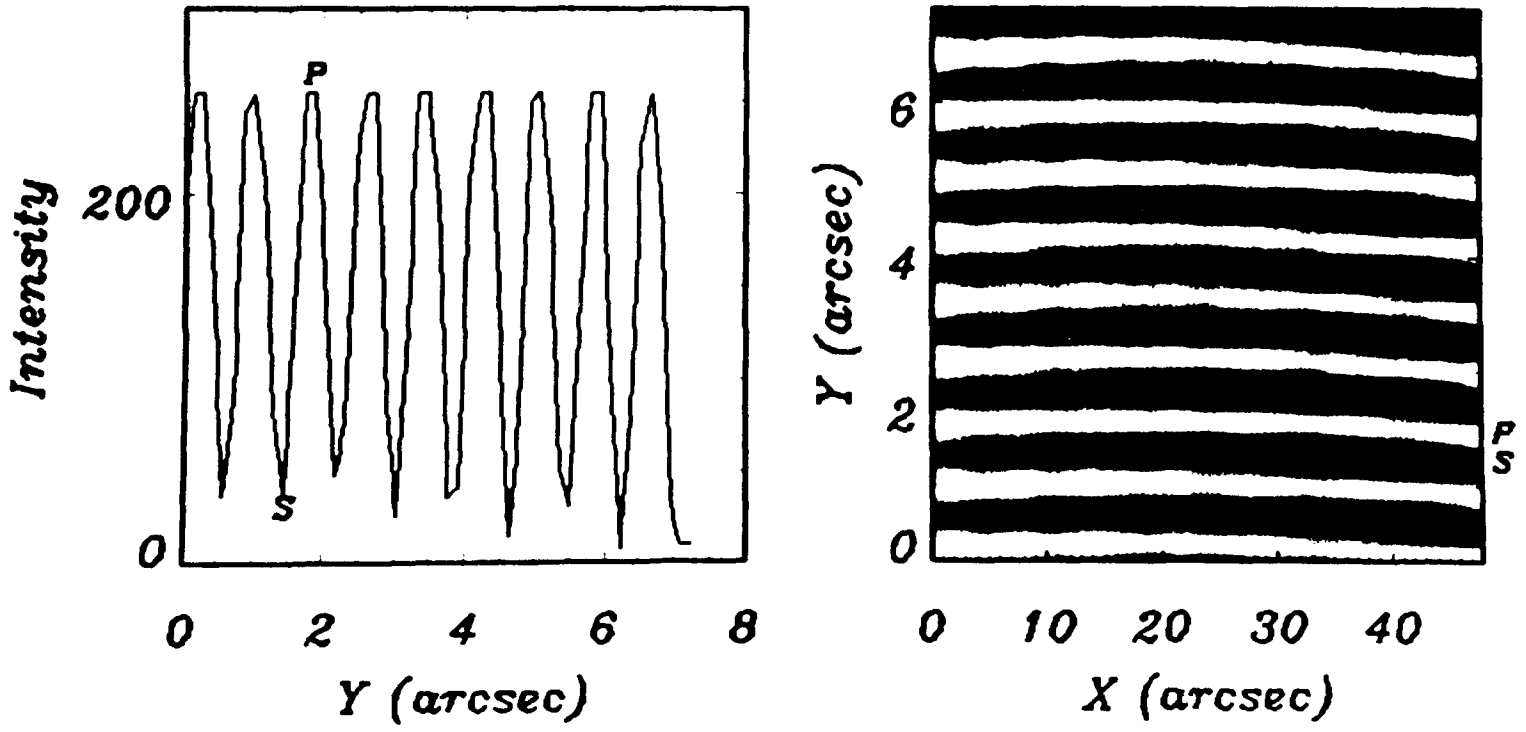

Fig. 3. The Venetian-blind pattern created in the detector plane during calibration.

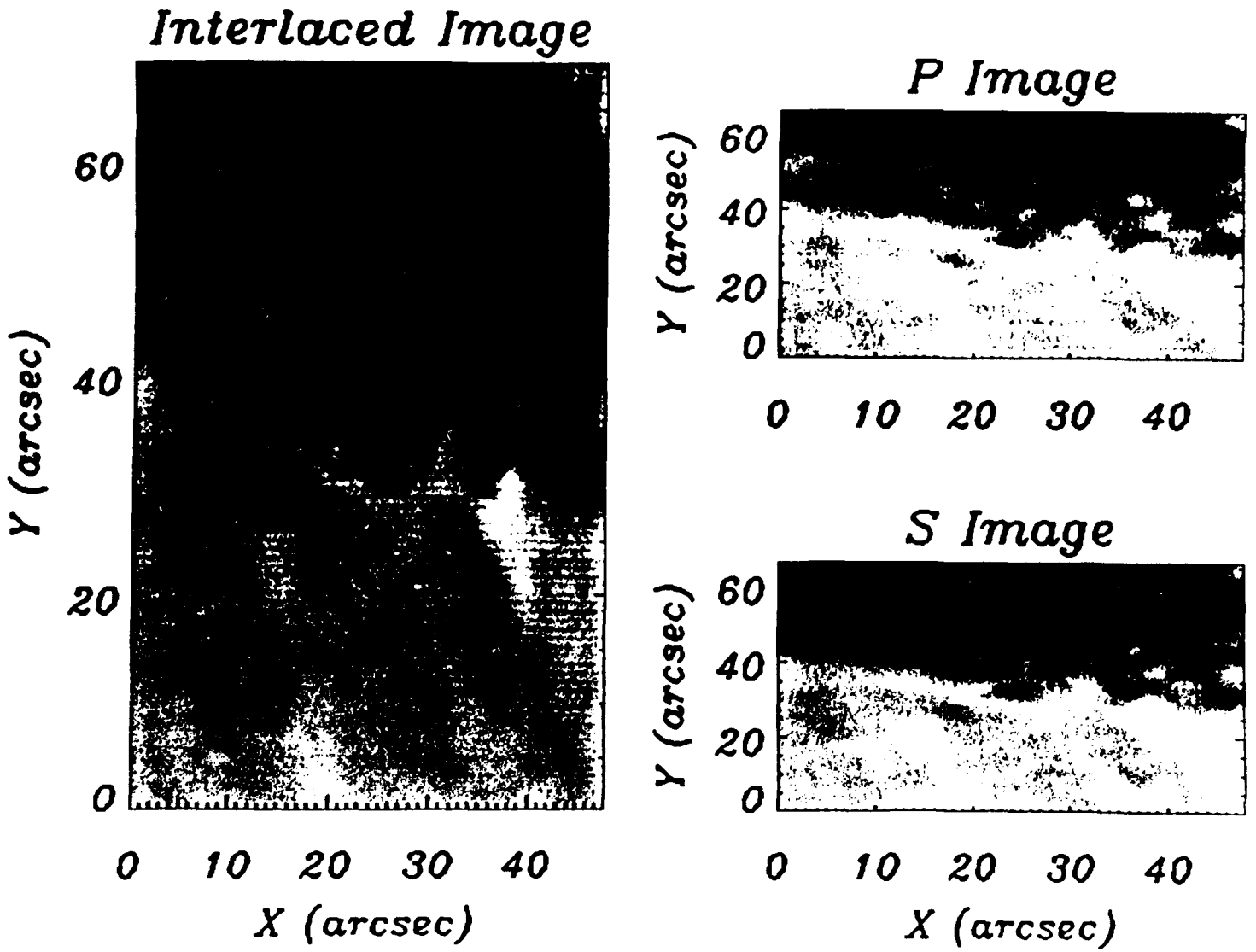

Fig. 4. Interlaced $\mathcal{P}$ and $\mathcal{S}$ images of a bomb at the outer edge of a penumbra on 2 August 1991, and the separated images. The linear polarization in the bomb was 5%.

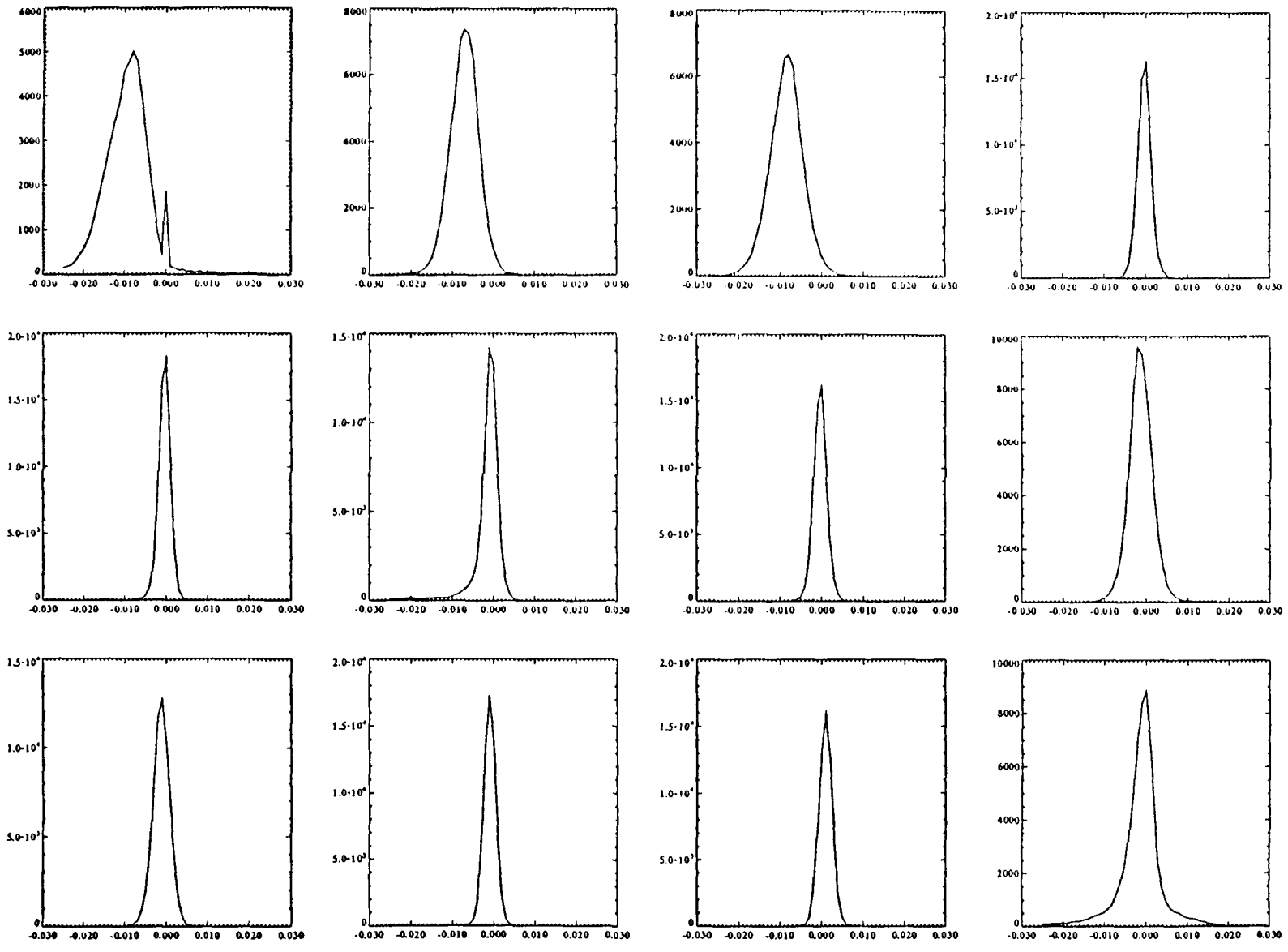

Fig. 5. Histograms of the twelve polarization maps before removal of the net (instrumental) polarization.

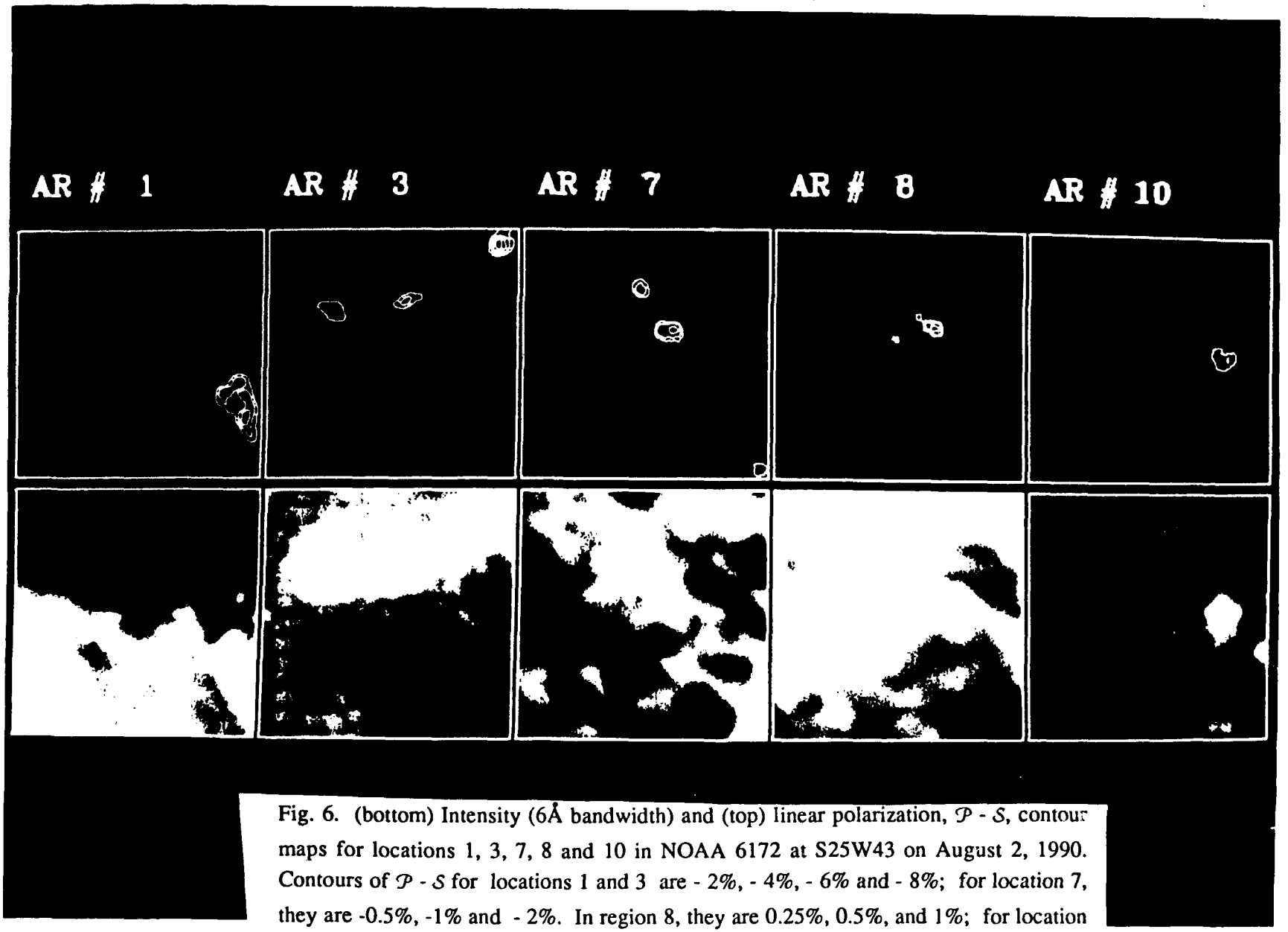

Fig. 6. (bottom) Intensity (6Å bandwidth) and (top) linear polarization, $\mathcal{P}$ - $\mathcal{S}$, contour maps for locations 1, 3, 7, 8 and 10 in NOAA 6172 at S25W43 on August 2, 1990. Contours of $\mathcal{P}$ - $\mathcal{S}$ for locations 1 and 3 are - 2%, - 4%, - 6% and - 8%; for location 7, they are -0.5%, -1% and - 2%. In region 8, they are 0.25%, 0.5%, and 1%; for location 10 (right), the contours represent 0.5% and 1% polarization.

Invited contribution to IAU Colloquium 133 "Eruptive Solar Flares, " Iguazu, Argentina, August 2 - 6, 1991. Proceedings will be edited by B. V. Jackson, M. E. Machado and Z. F. Svestka for publication by Springer Verlag in "Lecture Notes in Physics" series.

VARIATION OF THE VECTOR MAGNETIC FIELD IN AN ERUPTIVE FLARE

D. M. Rust
Johns Hopkins University Applied Physics Laboratory
Johns Hopkins Road, Laurel, Maryland, 20723 USA

G. Cauzzi
USAF Phillips Laboratory Geophysics Directorate
National Solar Observatory/Sacramento Peak
Sunspot, New Mexico 88349 USA

Summary

Observations of a 3B, M6 flare on April 2, 1991 appear to confirm earlier evidence that eruptive flares are triggered by measurable magnetic field changes. In the eight hours before the flare, the shear in the magnetic fields increased. The development that likely triggered the flare was the emergence into the active region and rapid proper motion of new flux. One of the small spots marking the negative magnetic leg of the new flux pushed into an established positive field at 0.2 km/s. Data from the JHU/APL vector magnetograph show that this motion led to the development of a sheared field. The flare started near the newly-sheared fields and spread to engulf most of the spot region. A magnetogram taken 45 min after flare onset shows possible relaxation of the sheared fields.

Introduction

We report here on observations of the vector magnetic fields in Active Region NOAA 6562 in which a two-ribbon 3B flare occurred on April 2, 1991, starting at 2251 UT. Flare maximum was at 2320 UT. The GOES X-ray classification was M6.1. On the basis of its long duration - more than 3 h - and the formation of prominent post-flare loops, we think this flare is a classic eruptive flare. H_α observations from the full-disk flare patrol at Sacramento Peak show some variation in the visibility of a thin filament between the two flare ribbons, but we cannot confirm from these films that there was a filament eruption. Nevertheless, all other indications are consistent with the usual sequence of events in an eruptive flare (Svestka 1976), including a Type IV metric radio burst that lasted for ~ 3 h. The flare was responsible for a three-day proton event at Earth. The flux of 10 MeV protons peaked at 52 pfu on April 4.

We obtained vector magnetic field observations at 1452, 1815, 2215, 2335, 2347 and 2355 UT on the day of the flare and on the previous day. The observations were made with the JHU/APL vector magnetograph (VMG) at Sacramento Peak (Rust and O'Byrne 1989, 1991).

Instrumentation

The VMG has a field of view of 2.4 arcmin x 3.6 arcmin. The detector is a 384 x 576-pixel CCD array, which sets the scale at 0.375 arcsec/pixel. We inferred the vector fields from filtergrams of $I + Q$, $I - Q$, $I + U$, $I - U$, $I + V$ and $I - V$ made in the 6122 Å line of Ca I. Stokes parameters I, Q, U, and V were measured sequentially at two positions in the blue wing of the line. The JHU/APL vector magnetograph obtains images at six sequential settings of a Glan-Laser prism and a quarter-waveplate: 0°, 90°, 45° and 135°, with the waveplate out, and 0° and 90°, with the waveplate in. Filtergrams were obtained at a rate of about 30/min. Ten twelve-image sequences were taken for each pair of interleaved magnetograms. The deleterious effects of poor seeing can be alleviated with an image motion compensator (Strohbehn 1990), but it was not operating during our observations.

The narrow-band filter in the VMG is a lithium niobate ($LiNbO_3$) Fabry-Perot etalon (Burton, Leistner and Rust, 1987). It has a spectral bandwidth of 167 mÅ. The etalon is made from a 75-mm diameter wafer of crystalline, Z-cut lithium niobate polished to a thickness of 220 μm and $1/400^{th}$ wave rms flatness. Dielectric coatings on the surfaces are 93% reflecting over a 6000 - 8000 Å band, but so far, we have operated only in the 6122 Å line. The filter is tuned by application of voltage to the filter faces, which have transparent conductive coatings. The tuning parameter is 0.4 mÅ/V.

Interpretation of Stokes Measurements

We interpreted our measurements by appeal to the so-called weak field approximation (WFA) Jefferies and Mickey (1991). In the past the WFA has been applied only when the ratio of the magnetic splitting $\Delta\lambda_B$ ($= \mu_\lambda B$) to the Doppler width $\Delta\lambda_D$ of the spectral line is small. Jefferies and Mickey greatly extended the range of the WFA by carefully examining the errors entailed in letting this ratio approach and even exceed unity. They concluded that the range of WFA validity can be larger than previously thought, when magnetograph measurements are made sufficiently far into the line wings. For λ6122, where $\Delta\lambda_D$ = 116 mÅ, we can apply the WFA to all our measurements for magnetic fields < 2000 G, with < 30% error (Cauzzi, 1991).

To calibrate the VMG to measure the longitudinal field component $B \cos\gamma$, we used

$$V = -\,\mu_\lambda B \cos\gamma \left(\frac{dI}{d\lambda}\right) \qquad (1)$$

where $dI/d\lambda$ is the slope of the line at the offset position $\Delta\lambda_{off}$ of the passband from line center and γ is the zenith angle of the field B.

In calibrating the VMG, we applied a voltage $\mathcal{E}_{cal}$ to the etalon. (For the Ca I line, $(B \cos\gamma)_{cal}(Gauss) = 13\ \mathcal{E}_{cal}$, where $\mathcal{E}_{cal}$ is expressed in volts.) To get $(B \cos\gamma)_{measured}$

from $(B \cos \gamma)_{cal} (V_{measured}/V_{cal})$, the slope of the line, $dI/d\lambda$, should be the same for both calibration and observation. This means that the calibration should be performed on the same solar scene as the observations and that the calibration step $\Delta\lambda_{cal}$ should be small. We calibrated every measurement with $\Delta\lambda_{cal}$ = 20 mÅ, which simulates a 325 G longitudinal field.

Calibration of the Q and U signals is similar to the V calibration. According to Jefferies and Mickey (1991), the Stokes Q vector is given in the WFA by

$$Q = \left(\frac{\mu_\lambda B \sin \gamma}{2}\right)^2 \left(\frac{dI}{d\lambda}\right) \left(\frac{3}{\Delta\lambda_{off}}\right) \qquad (2)$$

where, $\Delta\lambda_{off}$ is the offset of the filter passband from spectral line center and the azimuthal factor has been suppressed. Q is proportional to the square of a simulated Zeeman shift over a wide range, for appropriate choice of $\Delta\lambda_{off}$. For calibration of the Q and U signals, then, one again introduces a passband shift in the etalon, now to simulate the apparent shift $\mu_\lambda B \sin \gamma$. The calibration of Q (and U) is done with the same $\Delta\lambda_{cal}$ and $dI/d\lambda$ as the measurements. The calibration sequences constitute a separate and independent set of magnetic measurements.

Because the flare occurred at N14° E00° (heliographic coordinates), we did not need to convert from an oblique view angle, as is usually necessary before commencing interpretations.

Results

We examined the VMG data for evidence of sheared fields and moving or emerging magnetic fields. Figure 1 shows the fields and sunspots in NOAA 6562 8 h before and 45 min after flare onset. The principal features of the AR were the southwestern cluster of large spots (lower right) with positive polarity and the eastern (left) cluster of large spots, also with positive polarity. The two clusters were very different, according to our vector magnetograms. Fields in the western cluster resembled potential fields, i.e., they point radially outward from the sunspots (Figure 2). The field direction in the eastern spots was nearly parallel to the boundary between the positive spots and the surrounding negative fields (on the left). Following the terminology of Hagyard *et al.* (1984), we call the fields sheared, and one might expect a flare to begin in this region.

The flare began, or was triggered, instead, in a large emerging flux region. Arrows in Figure 1 show the two spots A and B of this EFR. These spots separated at ~ 0.2 km/s in the 8 h leading up to the flare. Spot A, with negative field, drove rapidly southwestward while increasing in size and magnetic field strength. The effect of this motion was to steepen the horizontal gradient in the longitudinal field between spot A's leading edge and the small positive spot C just visible in the image at 2335 UT. This sort of activity has been noted before in large, carefully-examined flares (e.g., Gesztelyi, *et al.* 1989, Wang *et al.* 1991; Rust, Nakagawa, and Neupert 1975; Hoyng *et al.* 1981)).

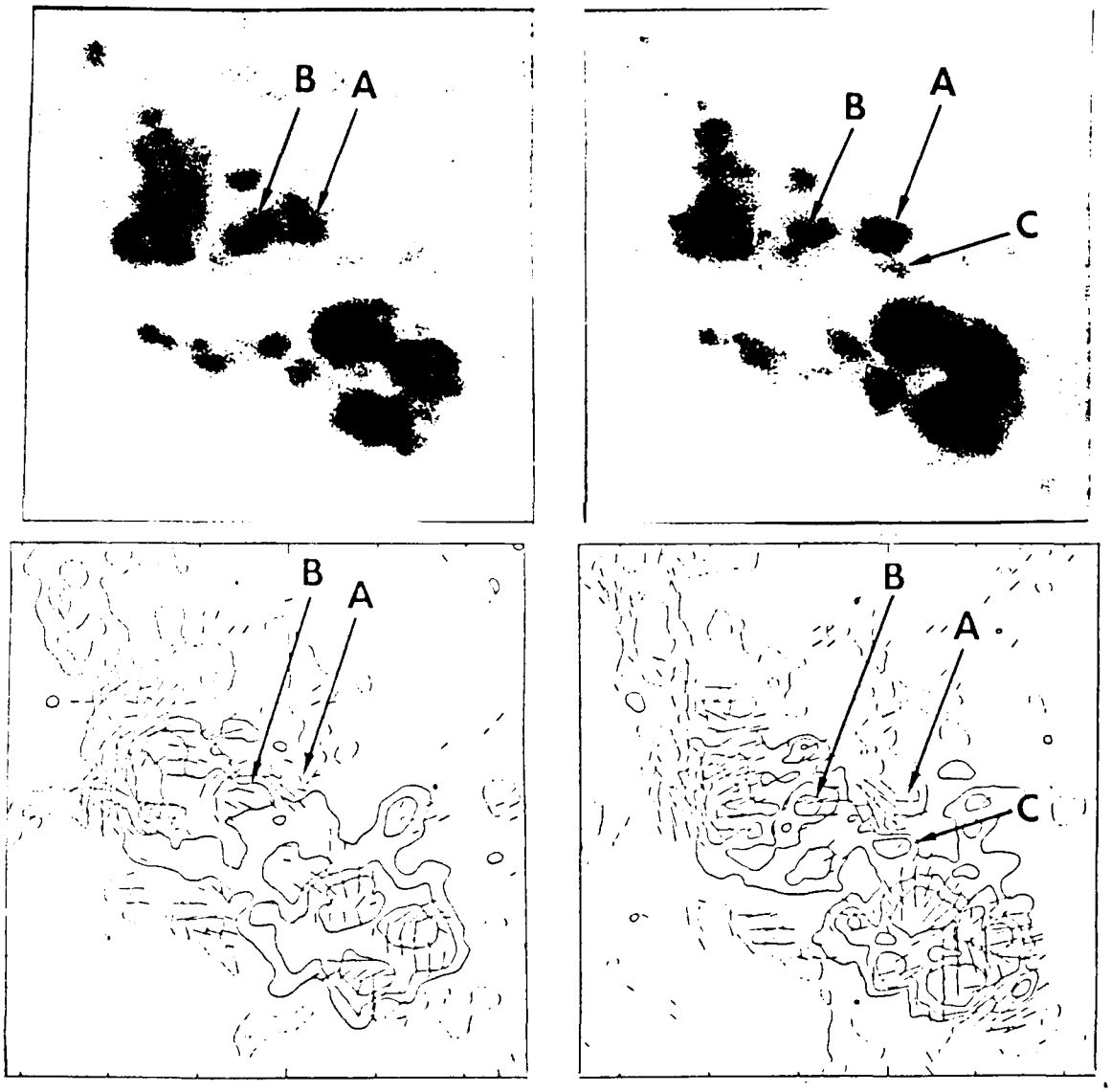

Figure 1. Filtergrams and magnetograms of AR NOAA 6562 on April 2 at 1455 UT (left) and 2330 UT (right). North is at the top, East is on the left. Arrows A and B show the EFR. The gradient in the longitudinal field steepened between A and C. Longitudinal field contours are 100, 400 and 800 G. Positive fields have solid contours, negative fields, dashed contours. Slashes represent transverse fields up to ~ 1600 G. Each image is 2.4 arcmin x 2.4 arcmin.

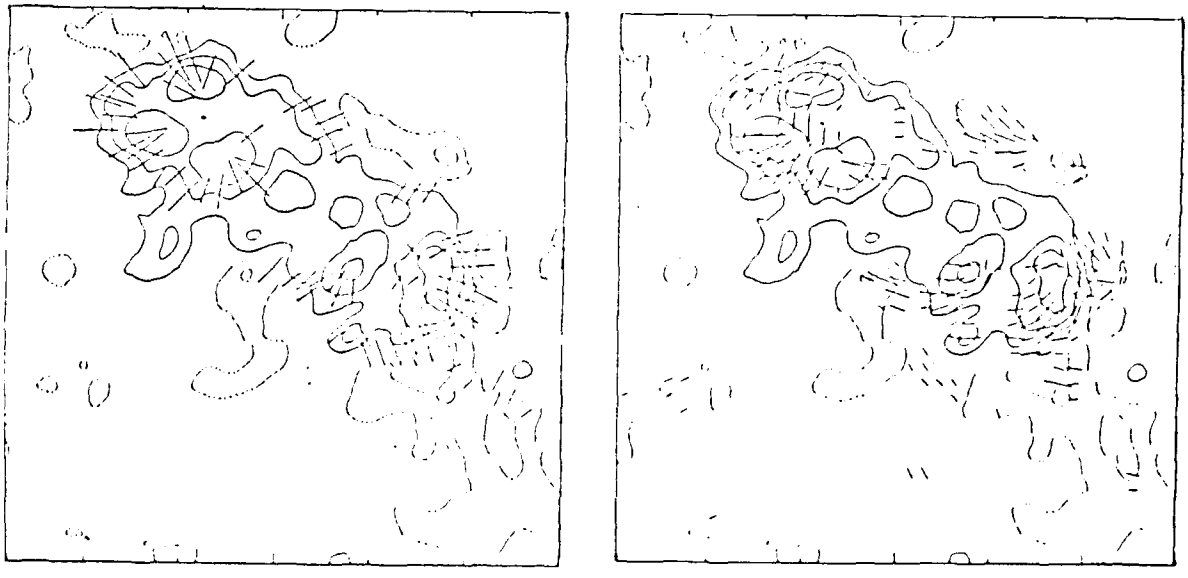

Figure 2. Comparison of the transverse component of the vector fields as measured at 1815 UT (left) and the transverse component as computed from the longitudinal fields under the assumption that no electric currents were present.

The vector magnetograms allowed us to see the effect of EFR growth and expansion on the transverse fields. Figure 3 shows, with independent magnetograms in two wavelengths, the transverse field in and near poles A and B of the EFR. These are linked by the arcade of slashes just to the left of center in the figure.

The observations at 1455 show transverse fields crossing the polarity boundary between A and C at ~ 90°. They resemble current-free fields. By 2215 UT, just 36 min before flare onset, the angle was closer to 0°. Thus, the observations show a build up of shear between A and C The lowest panels in Figure 3, taken at 2335 UT, shown a lessening of the shear.

The arrows in Figure 3 show a prominent transverse field that presented itself just before the flare, but it is not seen in any other magnetogram. It is tantalizing evidence for possible welling-up of new flux just before the flare.

High-resolution observations of the flare onset are not available, but the Sacramento Peak flare patrol images show early flare brightenings at A and C (Figure 1). Other areas in the region also brightened at about the same time. Unfortunately, the 60-s interval between exposures and the modest resolution of the images did not allow us to find the first flare kernels. We can say only that the flare may have started near the sheared region between A and C.

Conclusions

In agreement with earlier observations, e.g., Hagyard *et al.* (1984), we find that a large flare occurred near sheared fields. There were no flare ribbons near the leader spots, where the

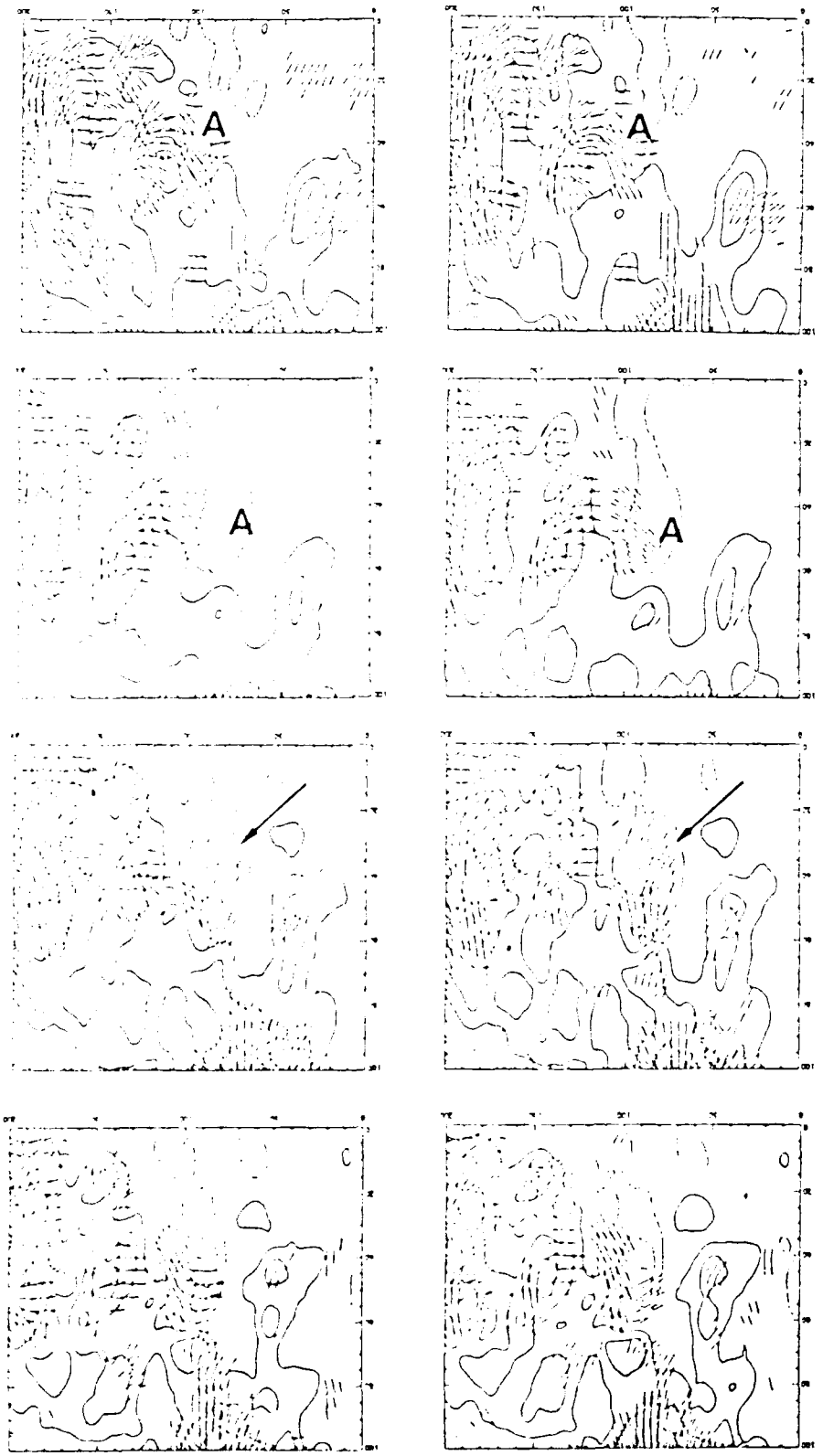

Figure 3. Two sequences of vector magnetograms in the region of the EFR. The series on the left was made with the filter at ~ 100 mÅ from line center. The sequence on the right, at 120 mÅ, was interleaved with the other, but it is an independent set of measurements. Observation times were (top to bottom) 1452, 1815, 2210 and 2335 UT.

vector fields most resembled current-free fields. However, the six magnetograms obtained before and after flare onset on April 2 have highlighted important developments that observations made only once per day could not show. The April 2 data illuminate earlier classic observations of sunspot motion and flux emergence. They show that an EFR can create a sheared field in < 8 h. High-resolution H_α observations have long been interpreted in just such terms (e.g., Rust, Nakagawa and Neupert 1975), but actual transverse field measurements showing the shear were not available until now.

No large flares except the one studied here occurred in AR6562. Yet, observations on the day before the flare showed that the sheared fields seen in the northeast on April 2 were present even then, although they were weaker. Hence, we must agree with Hagyard and Rabin (1986) that strongly sheared fields may be necessary for flares, but they are not sufficient. Some "external" perturbation is required to destabilize them. We think this destabilization may be related to reconnection of the emerging flux with the established fields. Just before the flare, a strong transverse field made a sudden and brief appearance near spot A. Could this have been the real trigger of the flare? More observations are needed, but it is entirely possible that fields from below the surface could emerge in ~ 45 min and disturb the previous equilibrium.

Acknowledgements

We are grateful to Craig Gullixson for operating the vector magnetograph. This work was sponsored by the Air Force Office of Scientific Research, grant AFOSR-90-0102. G. C. held an NRC Fellowship at the USAF Phillips Laboratory during the course of this work.

References

Burton, C. H., Leistner, A. J. and Rust, D. M. 1987: *Instrumentation in Astronomy VI*, SPIE Conf. Proc. **627**, 39 - 49.
Cauzzi, G. 1991: *NSO Technical Report 1991-01*, National Solar Observatory, Sunspot, NM.
Gesztelyi, L, Karlicky, M., Farnik, F., Gerlei, O., and Valnicek, B. 1986: in *The Lower Atmosphere of Solar Flares* (D. F. Neidig, ed.), Natl Solar Obs., Sunspot, p. 163.
Hagyard, M. J., Smith, J. B., Teuber, D., and West, E. A. 1984: *Solar Phys.* **91**, 115.
Hagyard, M. J. and Rabin, D. M. 1986: *Adv. Space Res.* **6** 7.
Hoyng, P., Frost, K. J., Woodgate, B. E., and the SMM HXIS Team 1981: *Astrophys. J. Lett.* **246**, L155.
Jefferies, J. and Mickey, D. L. 1991: *Astrophys. J.* **372**, 694.
Rust, D. M., Nakagawa, Y., and Neupert, W. 1975: *Solar Phys.* **41**, 397.
Rust, D. M. and O'Byrne, J. W. 1989: in *High Spatial Resolution Solar Observations*, D. Neidig (ed.), National Solar Observatory, Sunspot, NM, p. 378.
Rust, D. M. and O'Byrne, J. W. 1991: in *Solar Polarimetry*, L. November (ed.), National Solar Observatory, Sunspot, p. 74.
Strohbehn, K. 1990: *JHU/APL Tech. Memo. S1A-67-90*, JHU Applied Physics Laboratory, Laurel.
Svestka, Z. 1976: *Solar Flares*, Reidel, Dordrecht, p. 6.
Wang, H., Tang, F., Zirin, H., and Ai, G. 1991: *Astrophys. J.* (in press).